

For a particular RX, the rates uniformly follow the order $\text{Cl} < \text{Br} < \text{I}$. We have attempted to rationalize it in Figure 3 where the experimental hardnesses of Cl, Br, and I (Table III) are plotted against the respective values of $\log k_0$. Though it has been pointed out very recently that in the neutral ground-state electronegativity of an atom is proportional to its hardness,²⁶ we have chosen to use the hardness parameter to obtain an understandable physical picture: the less hard or more polarizable a group is, the lower the activation energy or the better the leaving group ability.

Similar trends are observed for vitamin B_{12s} also (Tables III and IV; Figures 3 and 4). The ρ values obtained from Figure 4 for Cl and Br are comparable -20.22 and 16.49 respectively. In Figure 3 the slopes of the lines in the two cases are almost same (3.83 ± 0.04). These results only corroborate the earlier notion⁴ that the kinetics of alkylation of the model complex and the vitamin B_{12s} are similar in a semiquantitative manner. We find the ρ_{av} value obtained from Figure 1 (14.61) is slightly less than that obtained in Figure 4 (18.35). This may be correlated with the difference in the nucleophilicities of the two systems⁴—vitamin B_{12s} being a stronger nucleophile than the model system.²⁷

In conclusion, we feel that the various features revealed here should be the general features of any oxidative-addition reaction. However, detailed theoretical calculations on model oxidative-addition reactions can help explore the real meaning of the present correlations.

Acknowledgment. The authors are indebted to Prof. J. Halpern for helpful advice regarding the manuscript. Thanks are also due to Prof. A. Chakravorty of IACS, Calcutta 700 032, India, for his kind interest. We thank reviewers for their constructive criticisms—especially the one who pointed out ref 7, 8, and 25.

Note Added in Proof. The values of a and b (Table II, Table III, and Figure 3) are in electronvolts.

Registry No. Vitamin B_{12s}, 18534-66-2; tributylphosphine-cobaloxime, 18475-26-8.

(26) Nalewajski, R. F. *J. Phys. Chem.* **1985**, *89*, 2831. Yang, W.; Lee, C.; Ghosh, S. K. *J. Phys. Chem.* **1985**, *89*, 5412. Datta, D. *J. Phys. Chem.* **1986**, *90*, 4216.

(27) It should be mentioned in this context that the nucleophilicity of cobaloxime, depends⁴ on its axial base, which is tributylphosphine in the chosen model system.¹⁰

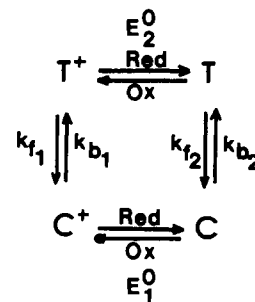
Contribution from the Laboratoire de Chimie Analytique et Appliquée, Faculté des Sciences Mirande, 21004 Dijon Cédex, France, and Laboratoire de Synthèse et d'Electrosynthèse Organométalliques associé au CNRS (UA 33), Faculté des Sciences, 21100 Dijon, France

Electrochemical Study of Thermodynamics and Kinetics of the Cis-Trans Isomerization of Dicarboxylbis[1,2-bis(diphenylphosphino)ethane]molybdenum and -tungsten Complexes and Their Cations

A. Vallat,*† M. Person,† L. Roullier,‡ and E. Laviron*‡

Received February 18, 1986

Certain organometallic complexes can exist in two different forms, either because of a configurational change (e.g. cis-trans or *fac-mer* isomerization) or because of a ligand exchange. When the oxidation state of the metal can vary, the situation can be described¹⁻⁶ by using the square scheme first proposed by Jacq⁷ or variants thereof.⁶ An example relative to a cis-trans isomerization and definition of the equilibrium constants are given in Figure 1.



$$K_1 = ([\text{C}^+]/[\text{T}^+])_{\text{equil}} = k_{f1}/k_{b1}$$

$$K_2 = ([\text{C}]/[\text{T}])_{\text{equil}} = k_{f2}/k_{b2}$$

Figure 1. The square scheme with definition of equilibrium constants. E_1° and E_2° are the standard potentials, E_1° being more positive than E_2° .

A general theory of the square scheme has been developed by Jacq⁷ in the case of the potentiostatic stationary method on a rotating disk electrode, but it is too complex to be used practically. When the electrochemical reactions can be considered at equilibrium, which is generally the case for organometallic compounds, the situation becomes simpler, but even then the mathematical resolution of the problem remains difficult. A partial solution was given by Bond and Oldham⁸ for the potentiostatic method on an immobile planar electrode, and simulations have been made by Evans,⁹ but these methods do not allow a complete analysis of the results to be carried out. The equilibrium constants can be determined only when the equilibria do not lie too far in one direction, e.g. by using spectroscopic^{6b} or voltammetric^{2h} methods. The analysis of the square scheme is thus often restricted to the measurement of the rate constants k_{f2} and k_{f1} .

In a recent publication,¹⁰ we have shown that the system can be completely analyzed; i.e., the equilibrium and rate constants can be determined by using electrochemical methods. When the ratio of the rate constants of the chemical reactions to the sweep

- (1) (a) Rieke, R. D.; Kojima, H.; Ofele, D. *J. Am. Chem. Soc.* **1976**, *98*, 6735. (b) Pilloni, G.; Zotti, G.; Corvaja, C.; Martelli, M. *J. Electroanal. Chem. Interfacial Electrochem.* **1978**, *91*, 385. (c) Rader, R. A.; McMillin, D. R. *Inorg. Chem.* **1979**, *18*, 546. (d) Moraczewski, J.; Geiger, W. E. *J. Am. Chem. Soc.* **1979**, *101*, 3407.
- (2) (a) Bond, A. M. *J. Electroanal. Chem. Interfacial Electrochem.* **1974**, *50*, 285. (b) Bond, A. M.; Colton, R.; Jackowski, J. *J. Inorg. Chem.* **1975**, *14*, 274. (c) Bond, A. M.; Cotton, R.; McCormick, M. *J. Inorg. Chem.* **1977**, *16*, 155. (d) Bond, A. M.; Grabaric, B. S.; Grabaric, Z. *Inorg. Chem.* **1978**, *17*, 103. (e) Bond, A. M.; Darenbourg, D. J.; Mocellin, E.; Stewart, B. J. *J. Am. Chem. Soc.* **1981**, *103*, 6827. (f) Bond, A. M.; Carr, S. W.; Colton, R. *Inorg. Chem.* **1984**, *23*, 2343. (g) Bond, A. M.; Carr, S. W.; Colton, R. *Organometallics* **1984**, *3*, 541. (h) Bond, A. M.; Colton, R.; Kevekordes, J. E. *Inorg. Chem.* **1986**, *25*, 749.
- (3) Wimmer, F. L.; Snow, M. R.; Bond, A. M. *Inorg. Chem.* **1974**, *13*, 1617.
- (4) Bond, A. M.; Grabaric, B. S.; Jackowski, J. *J. Inorg. Chem.* **1978**, *17*, 2153.
- (5) (a) Mugnier, Y.; Moïse, C.; Laviron, E. *J. Organomet. Chem.* **1981**, *204*, 61; *Nouv. J. Chim.* **1982**, *6*, 197. (b) Fakhr, A.; Mugnier, Y.; Broussier, R.; Gautheron, B.; Laviron, E. *J. Organomet. Chem.* **1983**, *255*, C8.
- (6) (a) Faure, D.; Lexa, D.; Savéant, J. M. *J. Electroanal. Chem. Interfacial Electrochem.* **1982**, *140*, 269, 285, 297. (b) Lexa, D.; Reutien, P.; Savéant, J. M.; Xu, F. *J. Electroanal. Chem.* **1985**, *191*, 253. (c) Lexa, D.; Savéant, J. M. *Acc. Chem. Res.* **1983**, *16*, 235. (d) Savéant, J. M. *Acc. Chem. Res.* **1980**, *13*, 323.
- (7) Jacq, J. *J. Electroanal. Chem. Interfacial Electrochem.* **1971**, *29*, 149.
- (8) Bond, A. M.; Oldham, K. B. *J. Phys. Chem.* **1983**, *87*, 2492.
- (9) (a) Olsen, B. A.; Evans, D. H. *J. Am. Chem. Soc.* **1981**, *103*, 839. (b) Neta, P.; Evans, D. H. *J. Am. Chem. Soc.* **1981**, *103*, 7041. (c) Evans, D. H.; Busch, R. W. *J. Am. Chem. Soc.* **1982**, *104*, 5057. (d) Olsen, B. A.; Evans, D. H. *J. Electroanal. Chem. Interfacial Electrochem.* **1982**, *136*, 139. (e) Evans, D. H.; Xie, N. *J. Electroanal. Chem. Interfacial Electrochem.* **1982**, *133*, 367; *J. Am. Chem. Soc.* **1983**, *105*, 315. (f) Matsue, T.; Evans, D. H.; Agranat, I. *J. Electroanal. Chem. Interfacial Electrochem.* **1984**, *163*, 137.
- (10) Laviron, E.; Roullier, L. *J. Electroanal. Chem. Interfacial Electrochem.* **1985**, *186*, 1.

* Laboratoire de Chimie Analytique et Appliquée.

† Laboratoire de Synthèse et d'Electrosynthèse Organométalliques.

Table I. Data for the Complexes at 60 °C

	E°_1/V	E°_2/V	E°_K/V	$K_1 = (C^+/T^+)_{eq}$	$K_2 = (C/T)_{eq}$	K_{b1}/s^{-1} ($C^+ \rightarrow T^+$)	k_{f1}/s^{-1} ($T^+ \rightarrow C^+$)	k_{r2}/s^{-1} ($T \rightarrow C$)	k_{b2}/s^{-1} ($C \rightarrow T$)
Mo	0.224	-0.184	-0.040	10^{-4}	150	140	1.4×10^{-2}	8×10^{-2}	5.3×10^{-4}
W	0.180	-0.172	-0.032	6.2×10^{-4}	130	35	2.2×10^{-2}	2×10^{-1}	1.5×10^{-3}

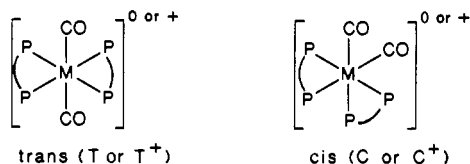
rate v becomes large enough,¹⁰ a single system of reversible redox peaks is obtained, with an apparent redox potential E°_K . If the equilibria are respectively in favor of T^+ and C , then¹⁰

$$E^{\circ}_K = E^{\circ}_1 - (RT/F) \ln(1 + K_1^{-1}) \quad (1)$$

$$E^{\circ}_K = E^{\circ}_2 + (RT/F) \ln(1 + K_2) \quad (2)$$

so that the equilibrium constants can be determined. When the sweep rate becomes faster, each half of the square scheme $T^+ \rightleftharpoons T \rightleftharpoons C$ and $C \rightleftharpoons C^+ \rightleftharpoons T$ can become¹⁰ equivalent to a reversible electrochemical reaction followed by an irreversible chemical reaction (EC scheme); the rate constants k_{r2} and k_{b1} can then be calculated with the help of known literature theories either by semiinfinite diffusion^{6b,10,11} or thin-layer linear potential sweep voltammetry.¹² In some cases, the system can behave in a more complex fashion¹⁰ and must be analyzed more completely with the help of the theory¹⁰ (see below). As shown theoretically in a previous paper,¹⁰ the cross-reactions $C + T^+ \rightleftharpoons C^+ + T$ does not participate in the kinetics of these reactions for this type of square scheme in thin-layer or semiinfinite diffusion cyclic voltammetry. The situation becomes different for a homogeneous process in solution, and evidence of the influence of the cross-reaction has indeed been presented recently¹³ in that case for other complexes.

In the field of configurational isomers of organometallic compounds, a pioneering work has been carried out by Bond et al.,²⁻⁴ who examined several series of complexes. Their results are however limited in most cases by the restrictions that we mentioned above. We study here one of the systems that they considered⁴ and that seemed appropriate for the illustration of the possibilities offered by our theory, viz. the complexes $cis-[M(CO)_2(DPE)_2]^+$ (C^+) and $trans-[M(CO)_2(DPE)_2]^+$ (T^+), in which $DPE = (C_6H_5)_2PCH_2CH_2P(C_6H_5)_2$ and $M = Mo$ or W ; they have been isolated as stable species.¹⁶



$trans-[Mo(CO)_2(DPE)_2]$ can be obtained by sodium amalgam reduction³ of the form T^+ ; it has been claimed that the C^+ form $cis-[Mo(CO)_2(DPE)_2]^+$ can be prepared chemically,¹⁴ but this was disproved later.¹⁵ Moreover, a qualitative study has shown that, in the case of the Mo complex, C can be oxidized to C^+ and T^+ reduced to T electrochemically,³ and it has been mentioned that the behavior of the tungsten complex is very similar.³

Experimental Section

Materials. $cis-[Mo(CO)_2(DPE)_2]$, $trans-[Mo(CO)_2(DPE)_2]^+ClO_4^-$ and $cis-[W(CO)_2(DPE)_2]$ were prepared according to literature procedures.¹⁶ $trans-[W(CO)_2(DPE)_2]^+ClO_4^-$, obtained by proceeding as for the trans Mo analogue, was prepared previously by another method.^{16c}

Instrumentation and Measurements. The electrochemical experiments were carried out in distilled DMF, THF, or Me_2SO , with 0.2 M tetra-

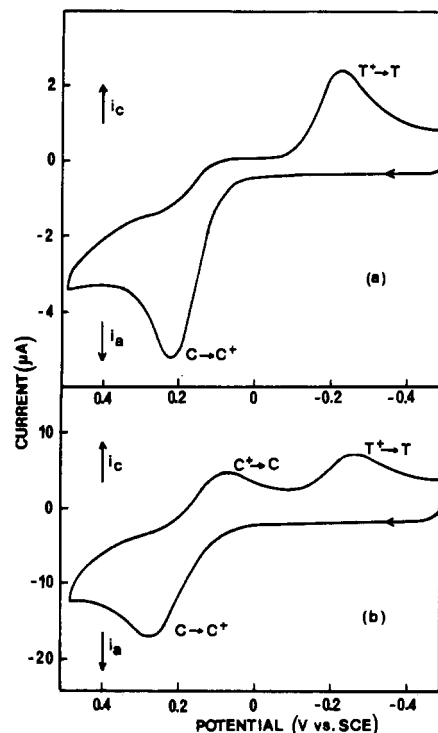


Figure 3. Voltammogram of $cis-[W(CO)_2(DPE)_2]$ (form C) in DMF at 60 °C with 0.2 M tetra-*n*-butylammonium perchlorate as supporting electrolyte (concentration 5×10^{-3} M dm^{-3}): (a) $v = 100$ V s^{-1} ; (b) $v = 1000$ V s^{-1} .

butylammonium perchlorate as supporting electrolyte. The potentials are relative to an aqueous saturated calomel electrode. The voltammograms were obtained by means of a UAP4 unit and a GSTP generator (Taccussel, Lyons, France); they were recorded on a Nicolet 3091 digital oscilloscope (Madison, WI) and subsequently reproduced on an XY recorder for fast sweep rates or recorded directly on the XY recorder for slow sweep rates.

In diffusion linear potential sweep voltammetry, a platinum disk electrode of small diameter (0.125 mm) was employed, in order to minimize the ohmic drop.¹⁷ Thin-layer cyclic voltammetry experiments were carried out with the cell described previously¹⁸ and a platinum electrode with a diameter of 2 mm.

Results

The results obtained in the three solvents DMF, THF, and Me_2SO are identical (see Discussion and Conclusion), and the behaviors of the Mo and W complexes are very similar. We will give as experimental examples those concerning the tungsten complex in DMF.

Determination of E°_2 . We will assume in what follows that the standard potentials are equal to the half-sum of the anodic and cathodic peaks. The error involved is small if the diffusion coefficients are not very different,¹⁹ as should be the case here. For reasons stated below (cf. paragraph on the determination of E°_K), we have carried out the measurements of E°_1 , E°_2 , and E°_K at 60 °C.

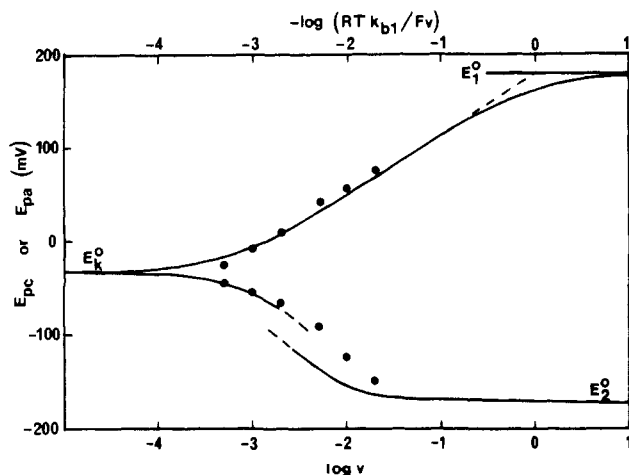
At moderately fast sweep rates (a few V s^{-1} at 60 °C), the T/T^+ system is reversible and E°_2 can easily be determined (Table I and Figure 2 (supplementary)).

- (11) (a) Nicholson, R. S.; Shain, I. *Anal. Chem.* **1964**, *36*, 707. (b) Savéant, J. M.; Vianello, E. *Electrochim. Acta* **1967**, *12*, 629.
 (12) Laviron, E. *J. Electroanal. Chem. Interfacial Electrochem.* **1972**, *39*, 1.
 (13) Connelly, N. G.; Raven, S. J.; Carriedo, G. A.; Riera, V. *J. Chem. Soc., Chem. Commun.* **1986**, 992.
 (14) (a) Reiman, R. H.; Singleton, E. *J. Organomet. Chem.* **1971**, *32*, C44. (b) Johnson, B. F. G.; Bhaduri, S.; Connelly, N. G. *J. Organomet. Chem.* **1972**, *40*, C36.
 (15) Snow, M. R.; Wimmer, F. L. *Aust. J. Chem.* **1976**, *29*, 2349.
 (16) (a) Chatti, J.; Watson, H. R. *J. Chem. Soc.* **1961**, 4980. (b) Crossing, P. R.; Snow, M. R. *J. Chem. Soc. A* **1971**, 610. (c) Lewis, J.; Whyman, R. *J. Chem. Soc.* **1965**, 5486.

- (17) Howell, J. O.; Wightman, R. M. *Anal. Chem.* **1984**, *56*, 524.
 (18) Vallat, A.; Laviron, E. *J. Electroanal. Chem. Interfacial Electrochem.* **1976**, *74*, 177.
 (19) Delahay, P. *New Instrumental Methods in Electrochemistry*; Interscience: New York, 1964; pp 120, 55.

Table II. Half-Sum of the Anodic and Cathodic Peak Potentials for the System C⁺/C

	$v/V \text{ s}^{-1}$			
	500	1000	2000	3000
Mo	0.222	0.222	0.223	0.224
W	0.177	0.181	0.179	0.182

**Figure 4.** Variations of the thin-layer peak potentials for *cis*-[W(CO)₂(DPE)₂] as a function of $\log v$ (v in $V \text{ s}^{-1}$) at 60 °C. The theoretical curve is calculated with $k_{b1}/k_{b2} = 2.3 \times 10^4$, $K_1 = 6.2 \times 10^{-4}$, $K_2 = 130$, and $E_1^0 - E_2^0 = 0.352 \text{ V}$ (see Table I).

Determination of E_1^0 . An example of oxidation peak for C is shown in figure 3a; even at relatively high sweep rates, no corresponding reduction peak $C^+ \rightarrow C$ is observed; instead, the peak corresponding to the reduction of T^+ to T appears. This shows that the oxidation of C to C^+ is followed by a fast isomerization of C^+ to T^+ . Only by raising the sweep rate above 250 $V \text{ s}^{-1}$ does the reduction peak of C^+ to C appear (Figure 3b). It can be deduced from the theory of Nicholson and Shain^{11a} that the half-sum of the oxidation and reduction peaks is practically equal to $E_{1/2}$ (E^0) as soon as the reduction peak is visible. This is what we have observed; the value obtained remains constant when the sweep rate is increased (Table II).

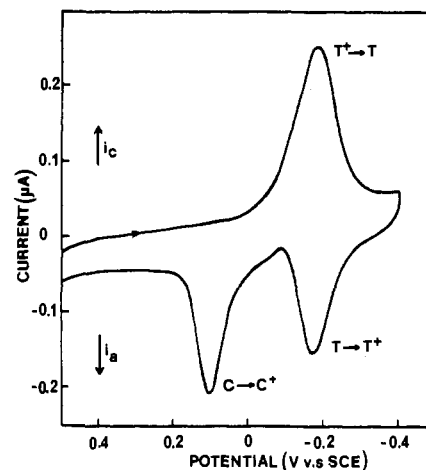
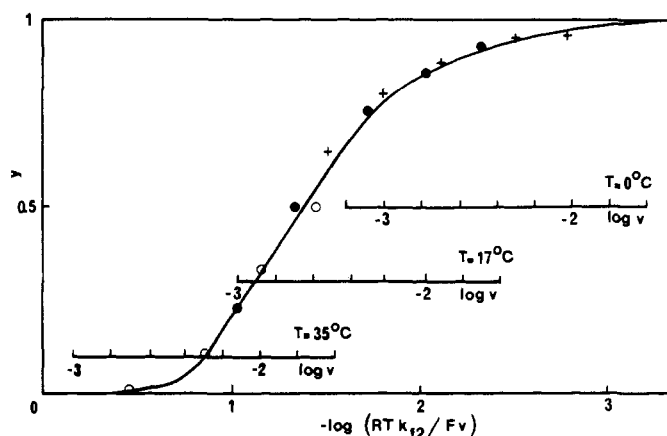
The average value for E_1^0 is given in Table I.

Determination of E_2^0 and Calculation of K_1 and K_2 . As mentioned in the introduction (cf. ref 10), at slow sweep rates the whole system is at equilibrium, and the whole reaction, starting from C to give T^+ or from T^+ to give C, appears reversible, giving a system of oxidation–reduction peaks centered at potential E^0_K . An example of variations of the anodic and cathodic peak potentials as a function of the logarithm of the sweep rate is shown in Figure 4 for thin-layer cyclic voltammetry.

The potentials are corrected for the ohmic drop by comparison with the peaks of the ferrocene–ferrocenium reversible couple under the same conditions. The diagrams have the shape expected;¹⁰ on the side of E_1^0 , the system behaves as an EC (irreversible) system, and the slope has the value predicted for a first-order reaction ($2.3RT/F$).^{10,12} We also verified that the same curves are obtained whatever the concentrations. On the side of E_2^0 , the shape of the curve is more complex, since two peaks appear (cf. Figure 7 of ref 10), but the variations conform to the theoretical predictions, except for a few points near E_2^0 . The potential E^0_K is attained for the lowest sweep rates that can be used with the cell that we employed;¹⁸ this explains why we had to carry out the determination at 60 °C. Below this temperature, E^0_K cannot be reached.

From eq 1 and 2, we deduce the values of K_1 and K_2 given in Table I.

Determination of k_{b1} and k_{f1} . As mentioned above, we have in that case an EC (irreversible) system for the reaction $C \rightleftharpoons C^+ \rightarrow T^+$. As the rate of the reaction is large (cf. Figure 3), we first contemplated using the theory of Nicholson and Shain^{11a} or Savéant and Vianello^{11b} in semiinfinite diffusion linear potential

**Figure 6.** Thin-layer voltammogram of *trans*-[W(CO)₂(DPE)₂]⁺ (form T⁺) in DMF at 25 °C with 0.2 M tetra-*n*-butylammonium perchlorate as supporting electrolyte (concentration $5 \times 10^{-4} \text{ M dm}^{-3}$; $v = 10 \text{ mV s}^{-1}$).**Figure 7.** Variations of y with $\log v$ (v in $V \text{ s}^{-1}$) for the redox system $T^+ \rightleftharpoons T$ (tungsten complex) in DMF. Conditions are the same as for Figure 6, except that v is changed. The full curve is the calibration curve; the points are the experimental values. The horizontal scales $\log v$ and $\log(RTk_{f2}/Fv)$ are made to coincide, and k_{f2} is calculated from their comparison (cf. ref 6). T : (O) 35 °C; (●) 17 °C; (+) 0 °C.

sweep voltammetry to determine k_{b1} . However, the lack of precision in measuring the height of the cathodic peak, owing to the large residual current and to the ohmic drop, precluded the use of their method, which is very sensitive to this type of effects. We obtained k_{b1} by thin-layer linear sweep voltammetry from the intersection of the asymptote of the curve $E_{pa} = f(\log v)$ with E_1^0 (Figure 4), which is such that at this point¹² $k_{b1} = Fv/RT$. The value of k_{b1} at 60 °C is given in Table I, together with the value of k_{f1} calculated from K_1 (Figure 1). The variations of $\log k_{b1}$ with $1/T$ are shown in Figure 5 (supplemental). The activation energies are 58 and 46 kJ for the Mo and W complexes, respectively.

Determination of k_{f2} and k_{b2} . At low sweep rates, the anodic peak of the system T/T^+ is no longer equal to the cathodic peak (Figure 6). Its height decreases, and the oxidation peak of C to C^+ appears at more positive potentials. The reaction $T^+ + e^- \rightleftharpoons T$ is followed by a slow isomerization of T to C. We have determined the value of k_{f2} at several temperatures by using the calibration curves $y = f(\log(RTk_{f2}/Fv))$ for a first-order EC (irreversible) reaction in thin-layer linear potential sweep voltammetry (Figure 7; cf. Figure 13 of ref 12), y being the ratio of the height of the anodic peak to that of the cathodic peak. The order of the reaction was established by varying the concentration; this has no influence on the ratio y . As mentioned above (determination of E^0_K), the system does not actually correspond to a simple EC (irreversible) reaction. However, we have calculated with the help of the theory of ref 10, by using the values of K_1 ,

Table III. Comparison of the Constants for the Two Complexes

	$K_2 = (C/T)_{eq}$	$K_1^{-1} = (T^+/C^+)_{eq}$	K_1^{-1}/K_2	k_{b1}/k_{f2}	k_{f1}/k_{b2}
Mo	150	10^4	66	1750	26
W	130	1.6×10^3	12	175	14

K_2 , k_{b1} , and k_{b2} , that the ratio y in the region around E°_2 remains practically the same as for an EC (irreversible) system (Figure 8, supplemental).

The variations of $\log k_{f2}$ with T^{-1} are shown in Figure 9 (supplemental). The activation energies are respectively 67 and 72 kJ for the Mo and W complexes; extrapolation gives the value of k_{f2} at 60 °C, and the value of k_{b2} is deduced from K_2 (Figure 1); see Table I.

Discussion and Conclusion

All the experiments reported above were repeated with THF and Me_2SO as solvents; the same quantitative results were obtained. Also, we introduced the ligand DPE into the solution at diverse concentrations, but this did not affect the constants. The cis-trans reaction is thus a process purely internal to the molecule. This conclusion was already reached by Bond et al.,⁴ who determined K_{f2} and k_{f1} in different solvents. The values they measured are comparable with ours, although the activation energies are somewhat different.

Our theory allows more complete information to be obtained about the complexes. The behaviors of the Mo and W complexes are analogous, although quantitative differences exist. First, if we compare K_1^{-1} to K_2 (Table III), we see that for both complexes the equilibrium is much more in favor of the stable form (T^+) in the couple C^+/T^+ than in favor of the stable form C in the couple C/T. However, from the ratio of K_1^{-1} to K_2 , it appears that the difference in stability is much larger in the case of the Mo complex (ratio 66 instead of 12).

On the other hand, for comparing the mobility of the reaction T^+/C^+ to that of the reaction T/C, we can compare k_{b1} to k_{f2} and k_{f1} to k_{b2} , respectively. The ratios obtained are always larger than 1 (they vary from 14 to 1750; Table III), which shows that the reaction $T^+ \rightleftharpoons C^+$ is faster in both directions than the reaction $T \rightleftharpoons C$ for both complexes. If now we compare the two complexes, we see that the difference in mobility of the two reactions is larger in the case of Mo than of W; the rate toward the more stable form T^+ is 10 times larger than that toward the stable form C ($k_{b1}/k_{f2}(\text{Mo}) = 10k_{b1}/k_{f2}(\text{W})$), whereas the rate in the reverse direction is about twice as fast in the case of Mo than in the case of W ($k_{f1}/k_{b2}(\text{Mo}) \approx 2k_{f1}/k_{b2}(\text{W})$).

Acknowledgment. We express our thanks to Professor A. Dormond for his help in the preparation of the complexes.

Supplementary Material Available: Figures 2, 5, 8, and 9, showing a voltammogram of the W cation (T^+ form), theoretical variations of the ratio y for the T^+/T couple in the square scheme for the W complex, and variations of $\log k_{b1}$ and $\log k_{f2}$ with T^{-1} for both complexes (4 pages). Ordering information is given on any current masthead page.

Contribution from the Department of Chemistry,
National Tsing Hua University, Hsinchu,
Taiwan 30043, Republic of China

Solvent Effects on Axial Ligation of Isomeric (5,7,7,12,14,14-Hexamethyl-1,4,8,11-tetraazacyclotetradeca-4,11-diene)copper(II) Cations with Mononegative Ligands

Jy-Wann Chen, Chi-Chang Chang, and Chung-Sun Chung*

Received April 19, 1986

The complex ion (5,7,7,12,14,14-hexamethyl-1,4,8,11-tetraazacyclotetradeca-4,11-diene)copper(II), $\text{Cu}(\text{Me}_6[14]4,11\text{-dieneN}_4)^{2+}$, can exist in two diastereoisomeric forms, $\text{Cu}(N\text{-rac-Me}_6[14]4,11\text{-dieneN}_4)^{2+}$ and $\text{Cu}(N\text{-meso-Me}_6[14]4,11\text{-dieneN}_4)^{2+}$, depending on the configurations of the two asymmetric nitrogen centers (see Figure 1). The crystal structures of these isomers have been determined by three-dimensional X-ray methods.^{1,2} Previously, we have reported the equilibrium constants for the reactions of these isomeric copper(II) complexes with several mononegative bases in aqueous solution represented by eq 1.³ Here L is the macrocyclic ligand $N\text{-rac-Me}_6[14]4,11\text{-dieneN}_4$ or $N\text{-meso-Me}_6[14]4,11\text{-dieneN}_4$. In order to study solvent effects on these ligation constants, the equilibria of these reactions in dimethylformamide (DMF), dimethyl sulfoxide (Me_2SO), and methanol (MeOH) were studied by spectrophotometric methods.

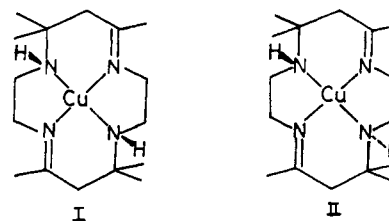


Figure 1. Structures of $\text{Cu}(N\text{-rac-Me}_6[14]4,11\text{-dieneN}_4)^{2+}$ (I) and $\text{Cu}(N\text{-meso-Me}_6[14]4,11\text{-dieneN}_4)^{2+}$ (II).

$\text{CuL}^{2+} + \text{X}^- \rightleftharpoons \text{CuLX}^+$ (1)

diene N_4 or $N\text{-meso-Me}_6[14]4,11\text{-dieneN}_4$. In order to study solvent effects on these ligation constants, the equilibria of these reactions in dimethylformamide (DMF), dimethyl sulfoxide (Me_2SO), and methanol (MeOH) were studied by spectrophotometric methods.

Experimental Section

Reagents. The macrocyclic complexes $\text{Cu}(N\text{-rac-Me}_6[14]4,11\text{-dieneN}_4)(\text{ClO}_4)_2$ and $\text{Cu}(N\text{-meso-Me}_6[14]4,11\text{-dieneN}_4)(\text{ClO}_4)_2$ were the same as those reported earlier.¹⁻³ The organic solvents, DMF, Me_2SO , and MeOH, used in this work were of spectroscopic grade. All other chemicals used were of GR grade from Merck.

Dimethylformamide was vacuum-distilled from phosphorus pentoxide. Dimethyl sulfoxide was dried over molecular sieves for 24 h and then refluxed over calcium hydride for 16 h; it was then carefully distilled under reduced pressure. Methanol was dried by fractional distillation, followed by treatment with Drierite for a period of several days.^{4,5}

Analysis of water in solvents was carried out by using an automatic Karl Fischer titrator. The water content of all purified solvents was found to be less than 100 ppm.

Instrumentation. A Cary 17 spectrophotometer and a Perkin-Elmer Lambda-5 UV/vis spectrophotometer with a thermostated cell compartment were used to record absorption spectra. The temperature was maintained within ± 0.1 °C. Equilibrium constants were obtained by a linear least-squares fit of the data using a CDC Cyber-172 computer.^{6,7}

Results

Addition of the solution of mononegative ligand, X^- , to a solution of copper(II) tetraaza macrocyclic complex results in the replacement of coordinated solvent by X^- . The apparent molar absorptivities were obtained by using eq 2, where A is the ab-

$$\epsilon_{app} = A/lC_T \quad (2)$$

sorbance of the solution, l is the length of the cell, and C_T is the total concentration of the copper(II) complexes, $[\text{CuL}^{2+}] + [\text{CuLX}^+]$. The values of apparent molar absorptivities for these systems as a function of $[\text{X}^-]_T$ are deposited as supplementary material (Tables A-C).

The apparent molar absorptivities have a linear dependence on $(\epsilon_{app} - \epsilon_{\text{CuL}})/[\text{X}^-]$ in accordance with eq 3, where ϵ_{CuL} and ϵ_{CuLX}

$$\epsilon_{app} = (-1/K_X)(\epsilon_{app} - \epsilon_{\text{CuL}})/[\text{X}^-] + \epsilon_{\text{CuLX}} \quad (3)$$

are the molar absorptivities of CuL^{2+} and CuLX^+ , respectively. The value of $[\text{X}^-]$ was calculated by an iterative procedure in which an estimated value of K_X was used to calculate the value

(1) Lu, T.-H.; Lee, T.-J.; Liang, B.-F.; Chung, C.-S. *J. Inorg. Nucl. Chem.* **1981**, *43*, 2333-2336.

(2) Lee, T.-J.; Lu, T.-H.; Chung, C.-S.; Lee, T.-Y. *Acta Crystallogr., Sect. C: Cryst. Struct. Commun.* **1984**, *C40*, 70-72.

(3) Wu, S.-Y.; Lee, C.-S.; Chung, C.-S. *Inorg. Chem.* **1984**, *23*, 2548-2550.

(4) Chen, C.-S.; Wang, S.-J.; Wu, S.-C. *Inorg. Chem.* **1984**, *23*, 3901-3903.

(5) Jolly, W. L. *The Synthesis and Characterization of Inorganic Compounds*; Prentice-Hall: New York, 1970; p 119.

(6) Lee, C.-S.; Chung, C.-S. *Inorg. Chem.* **1984**, *23*, 639-644.

(7) Lee, C.-S.; Chung, C.-S. *Inorg. Chem.* **1984**, *23*, 4162-4166.